Tomasz **MAKOWSKI**
Jarosław **DOMIN**

# cRIO-9022 AND myRIO-1900 CONTROLLER OUTPUT STATE CHANGE RATES

**Abstract.** The article compares some selected parameters of the cRIO-9022 (industrial controller) and myRIO-1900 (student device) from the point of view of their possible use in the electromagnetic launcher control system. The results of laboratory tests aimed at comparing the rise and fall time of the signal edge at the digital output for both controllers are presented. The study was conducted to assess the interchangeability of both controllers in the control system of a hybrid electromagnetic launcher with pneumatic assist.

**Keywords:** Controller, cRIO-9022, myRIO-1900, rise and fall time of signal edge, switching time.

## 1. CHARACTERISTICS OF cRIO AND myRIO DEVICES

### 1.1. General information

The CompactRIO (cRIO) and myRIO controllers belong to the RIO (Reconfigurable I/O) family of devices which feature an efficient and flexible architecture and which have been successively modernized during the last 10 years by National Instruments (NI) [6].

The RIO architecture integrates four components, presented graphically in Fig. 1: real-time processor, Field-Programmable Gate Array (FPGA) chips, modular inputs and outputs, and a complete software package for programming each block of the presented architecture [5], [6].

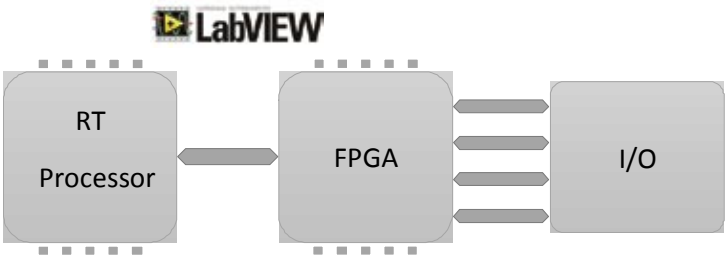


**Fig. 1. RIO architecture**

The LabVIEW software dedicated for RIO devices contains a set of built-in functions and algorithms. Programming the FPGA requires the use of low-level programming tools and hardware description language (HDL, VHDL, Verilog). RIO devices can be programmed intuitively using the G graphical language, which simplifies FPGA programming. It should be noted that LabVIEW software and National Instrument drivers are becoming more and more popular among engineers around the world [1], [3], [5].

### 1.2. Description of cRIO

The industrial CompactRIO controller, shown in Fig. 2, consists of: real-time controller (1), FPGA module (2), reconfigurable IO modules (3) and an integrated Ethernet

Tomasz **MAKOWSKI** – Ośrodek Badawczo-Rozwojowy Urządzeń Mechanicznych „OBRUM" sp. z o.o.
Dr Jarosław **DOMIN** – Silesian University of Technology, Gliwice

port (4). The standard device has 4 or 8 slots for I/O interface connectors (C Series modules), and this can be expanded using expansion slots [6].

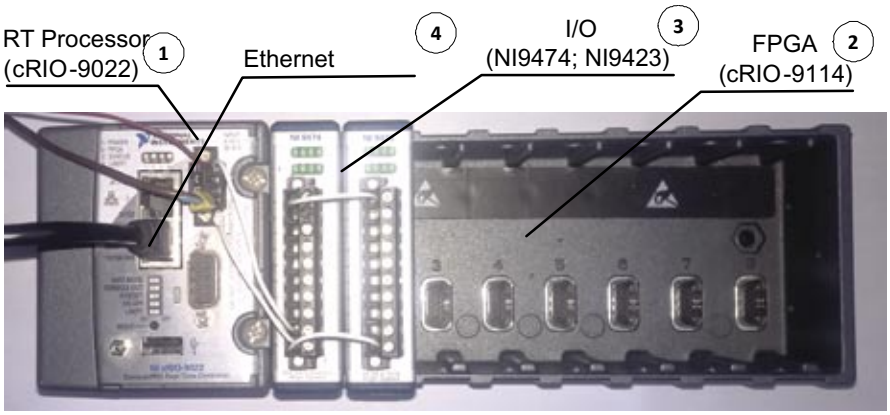


**Fig. 2. General view of the CompactRIO controller used**

The company now offers more than 150 types of C-Series modules, among them digital and analog input/output modules. There are also serial bus communication modules (RS232, RS485, RS422, LIN, CAN), motor controllers and safety modules. This series is designed for operation in an industrial environment. Table 1 shows the classification of modules according to selected parameters [4], [7].

**Table 1.** C Series modules according to selected parameters [4].

| C Series module type | Measured quantity | Maximum rate |
|---|---|---|
| Digital input | LVTTL, VTTL, 12 V, 24 V, 60 V, 0-50 V | 1 million operations/second |
| Digital output | LVTTL, VTTL, 12 V, 24 V, 30 V, 250 $V_{DC}$, 250 $V_{AC}$ | 1 million operations/second |
| Relays | 60 $V_{DC}$, 250 $V_{AC}$ | 1 operation/second |
| Analog voltage input | ±200 mV, ±500 mV, ±1 V, ±5 V, ±10 V, ±60 V, 3 $V_{rms}$, 300 $V_{rms}$, 400 $V_{rms}$, 800 $V_{rms}$ | 1 million operations/second/channel |
| Analog current input | ±20 mA, 5 $A_{rms}$, 20 $A_{rms}$, 50 $A_{rms}$, | 200 thousand operations/second |
| Analog universal input | V, mA, TC, RTD, Ω, IEPE | 51.2 thousand operations/second/channel |
| Analog voltage output | ± 10 V, ±40 V, 3 $V_{rms}$, | 1 million operations/second/channel |
| Analog current output | 20 mA | 100 thousand operations/second/channel |
| Temperature | Type: J, K, T, E, N, B, R, S, PT100, PT1000 | 400 operations/second |

| C Series module type | Measured quantity | Maximum rate |
|---|---|---|
| Strain – bridge based | ¼, ½, full bridge | 50 thousand operations/second/channel |
| Vibration and sound | ±5 V, ±30 V | 102.4 thousand operations/second/channel |

Despite the wide range of C Series modules, it may turn out that the module required for the target system does not exist. If this is the case, then there is a cRIO-9951 "Module Development Kit", which gives individual users the possibility to create their own C Series module. When creating a module, one should bear in mind the limitations related to mechanical and electrical requirements [8].

### 1.3. Description of myRIO

Like the cRIO, myRIO consists of: real-time system, embedded FPGA and, unlike the cRIO, built-in I/O interfaces (expansion not possible). It is designed mainly for instruction facilities and it may be implemented in basic industrial systems. [9], [14], [15].

There are two versions of myRIO: myRIO-1900 (Fig. 3) and myRIO-1950. The less expensive myRIO-1950 version has no enclosure and does not support Wi-Fi.

**Fig. 3. General view of myRIO-1900**

### 1.4. Comparison of the specifications of the controllers used

The rated parameters of the controllers selected for comparison (cRIO-9022 with the cRIO-9114 FPGA chassis and myRIO-1900) are summarized in Table 2.

The cRIO-9022 controller is now used as the main component of a test stand with a hybrid electromagnetic launcher with pneumatic assist. During the research work it was decided to consider the use of myRIO-1900 controller [2].

**Table 2.** Comparison between cRIO-9022 and myRIO-1900 [10], [11], [12], [14]

| Parameter | cRIO-9022 with cRIO-9114 and NI9474 | myRIO-1900 |
|---|---|---|
| RT processor frequency | 533 MHz | 667 MHz |
| FPGA processor: | Virtex-5 LX 50 40 MHz | Xilinx Z-7010 40 MHz |
| Digital output update rate | 1 µs | - |
| Digital output voltage range | 5 V to 30 V | 3.3 V or 5 V |
| Nonvolatile memory | 2 GB | 512 MB |
| DRAM memory | 256 MB | 256 MB |
| Clock accuracy | 200 ppm, 35 ppm at 24°C | - |
| Power supply | 9 V-35 V 55 W (17 W controller alone) | 6 V-16 V 14 W |
| Internet communication | 2 Ethernet ports expandable with modules | Wireless IEEE 802.11 b,g,n |
| Operating temperature | -20°C … +55°C | 0°C … 40°C |
| Ingress protection IP | IP40 | - |
| Inputs/outputs | Any number and any configuration, depends on modules used | Defined in device (see [14]) |

## 2. VERIFICATION MEASUREMENTS OF cRIO AND myRIO TRIPPING RATES

### 2.1. General measurement information

The controllers selected for comparison have different processors, which may cause differences in the switching times of the digital output. In order to compare the switching times, two identical programs were created in the LabVIEW environment, the task of which was to control one digital output, assuming that the other I/O modules remained inactive. The tests were carried out under identical atmospheric conditions, the controllers were next to each other, and the measurement was recorded at the same time. Measurement results were recorded on a Tektronix MDO3012 oscilloscope with a Tektronix TPP0250 probe at sampling frequency of 100 MHz. The obtained measurement results are presented and discussed in section 2.2 (rate of state change of digital output at no load controlled by FPGA only), section 2.3 (digital input switching time with output state tripped by FPGA) and section 2.3 (digital input switching time with output state tripped by RT processor).

### 2.2. Rate of state change of digital output at no load tripped by FPGA only

Controlling the digital output by FPGA allows bypassing the processes associated with data transfer between the FPGA and the RT processor. Both controllers selected for the study operate at the same frequency, therefore the comparison of the change rate of the digital output state depends only on the signal output switching system used by the manufacturer.

The programs developed (Fig. 4), applied for both controllers, were written in the G language in the LabVIEW environment. The main part of the program is a "while" loop which cycles the output state.. In addition, a "wait" function was inserted in the loop to delay the execution of the loop for a specified time.

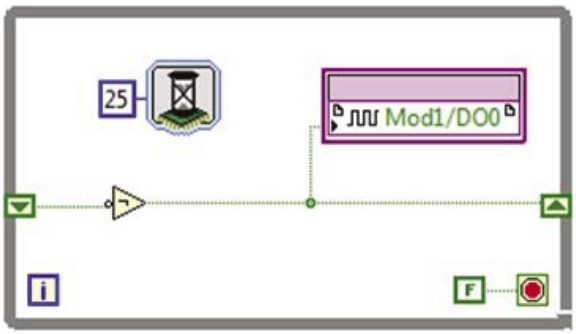


**Fig. 4. Program for testing the change rate of digital output state – generator**

In the first stage, changes of the output state for the generated signal were tested at a switching frequency of 40 Hz (cyclical change of the output state every 25 ms). The waveforms recorded for cRIO and myRIO are shown in Fig. 5 and Fig. 6, respectively.

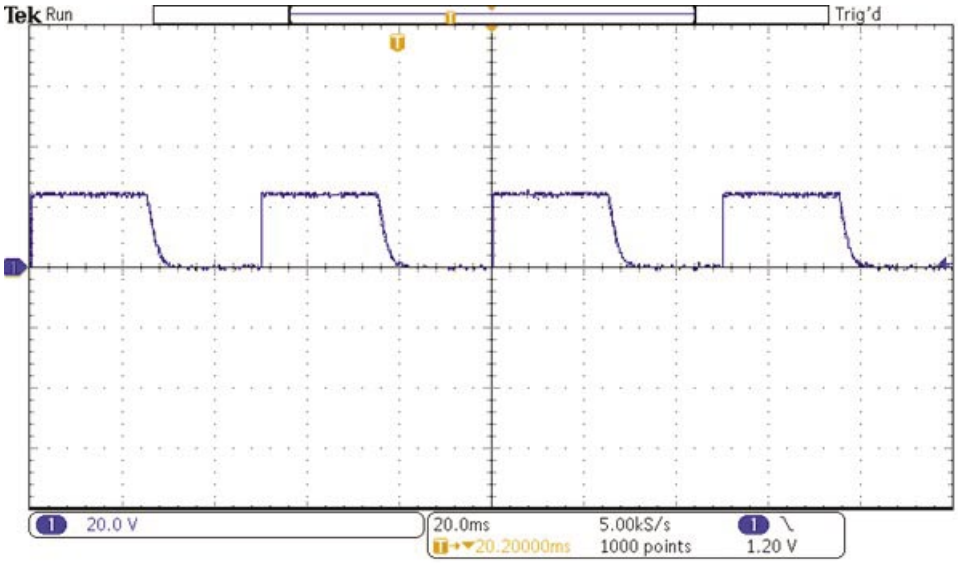


**Fig. 5. Result of cRIO output testing at 40 Hz**

The changes of the controller output state with time shown in Fig. 5 indicate that during the switching of the signal a falling edge with a time constant of 8 ms is observed. In

order to eliminate the falling edge, an additional resistance must be placed between the tested output and the ground.

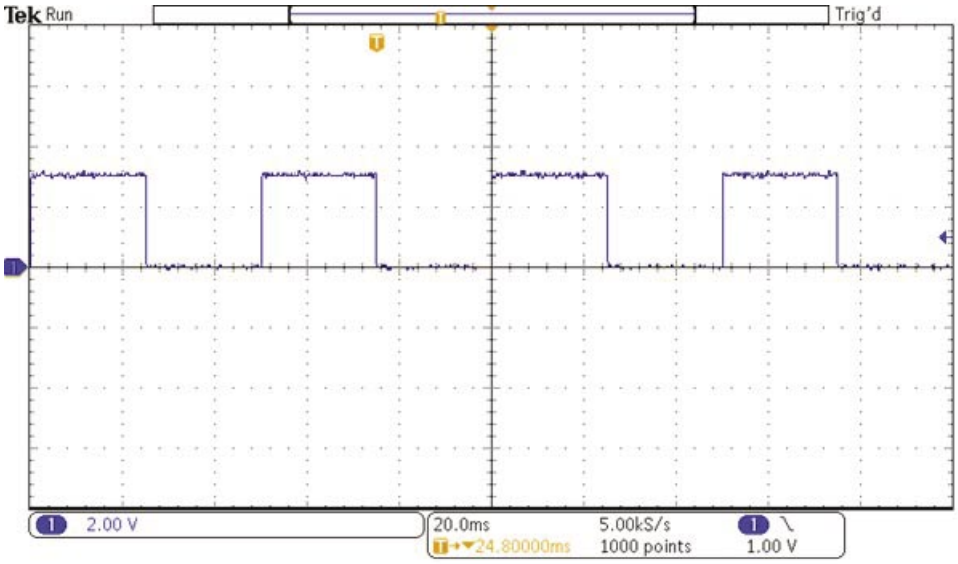


**Fig. 6. Result of myRIO output testing at 40 Hz**

In the next step testing was carried out with the switching frequency of 1 kHz (1 ms). The waveforms recorded for cRIO and myRIO are shown in Fig. 7 and Fig. 8, respectively.

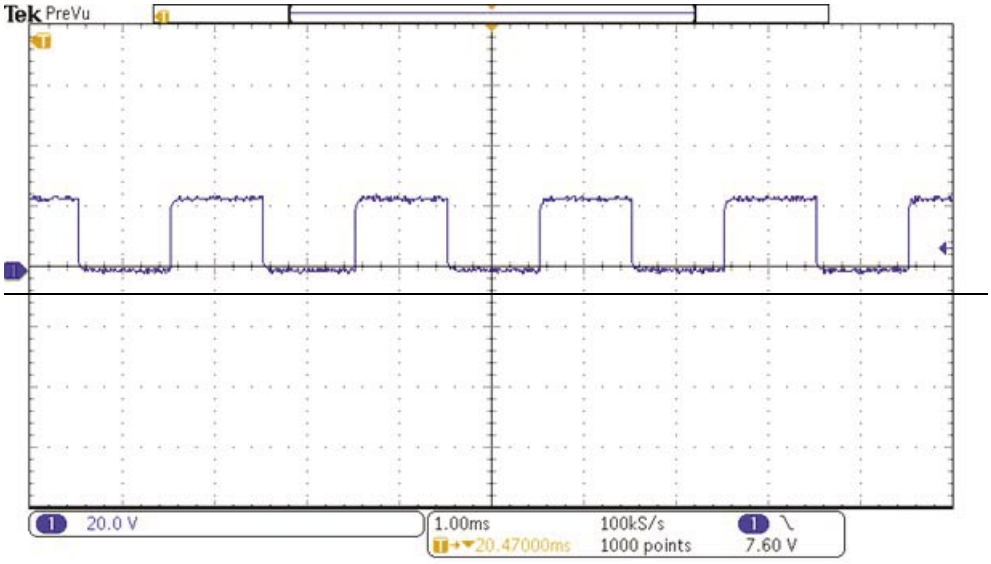


**Fig. 7. Result of cRIO output testing at 1 kHz**

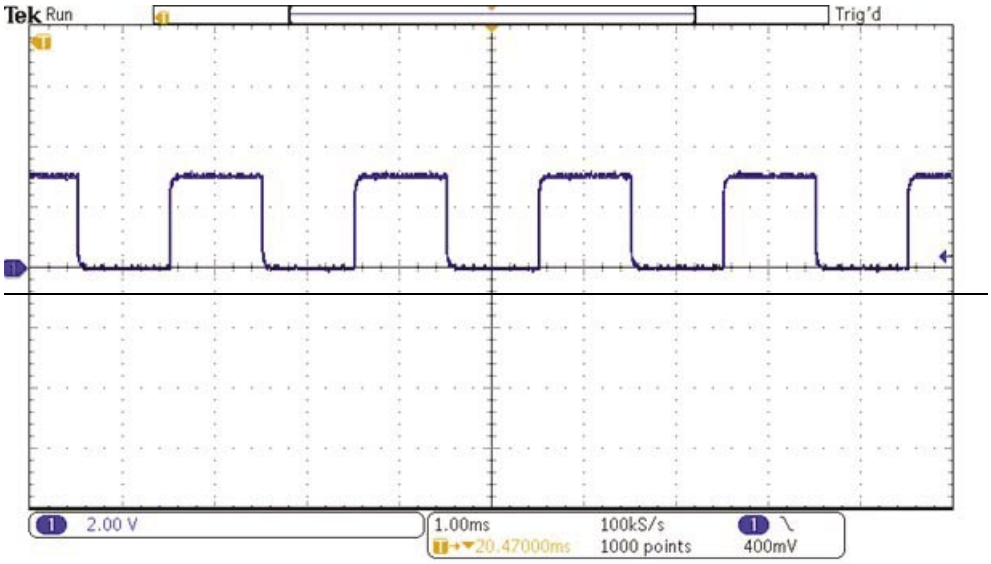


**Fig. 8. Result of myRIO output testing at 1 Hz**

The obtained results are satisfactory (the signal is characterized by a 50% duty cycle and there are no interferences that would prevent proper operation of the controller in the hybrid launcher control system). In the next step the switching frequency was increased to 1 MHz (1 µs). The waveforms recorded are shown in Fig. 9 (cRIO) and Fig. 10 (myRIO).

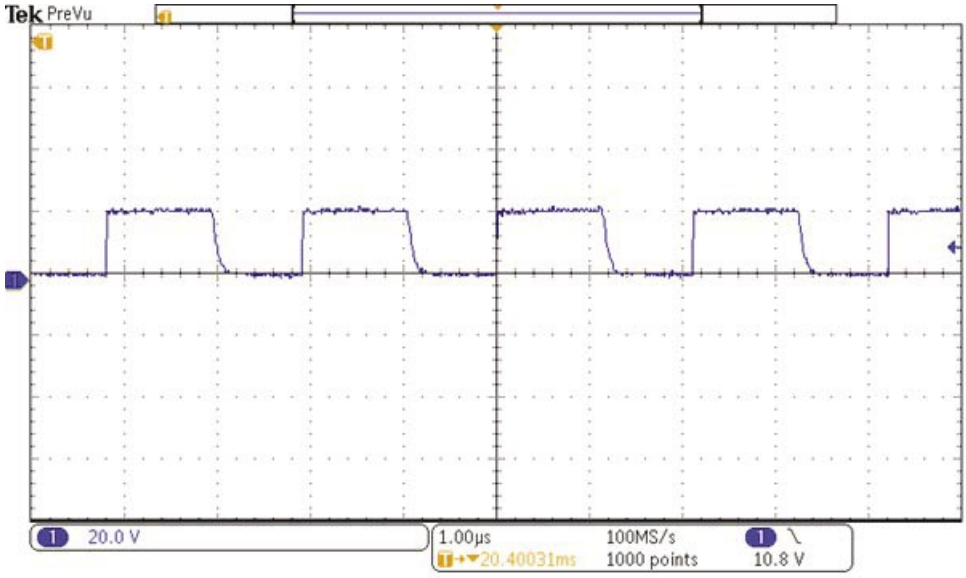


**Fig. 9. Result of cRIO output testing at 1 MHz**

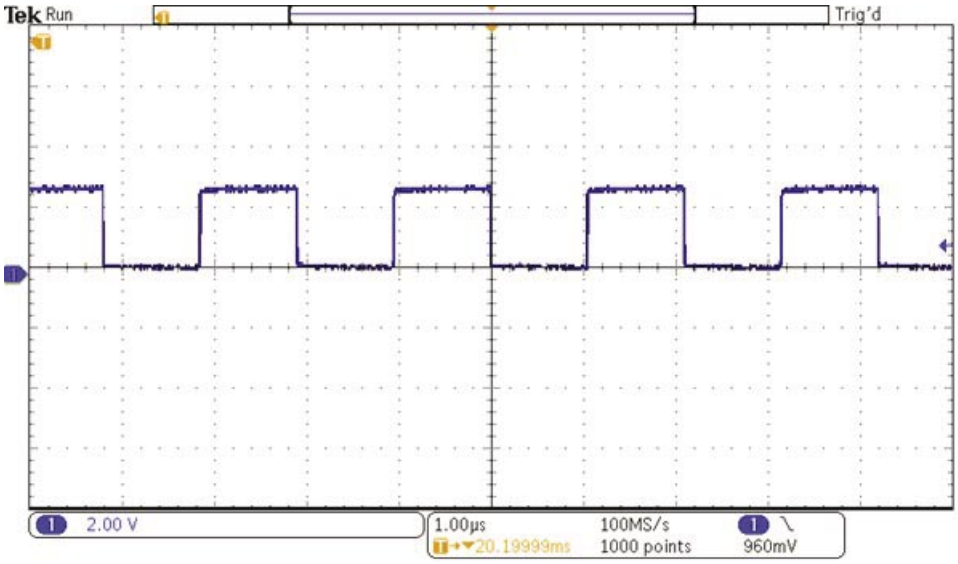


**Fig. 10. Result of myRIO output testing at 1 MHz**

The illustrations show that the deviations from the set conditions (switching at 1 MHz) are minimal. Moreover, a falling edge is observed again at the cRIO output. Despite the distortion of the signal at the 1 MHz switching frequency, the results are considered satisfactory, as they still ensure correct operation of the hybrid launcher.

In the next stage, the output state was tested without introducing delays (no "wait" function). The waveforms recorded for cRIO are shown in Fig. 11, and for myRIO in Fig. 12.

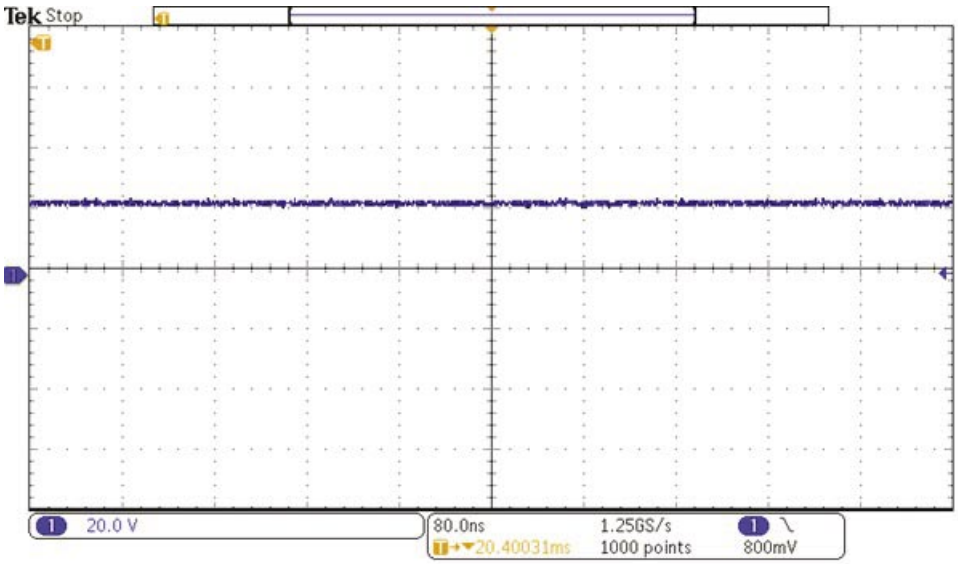


**Fig. 11. Result of cRIO output testing with no delay time**

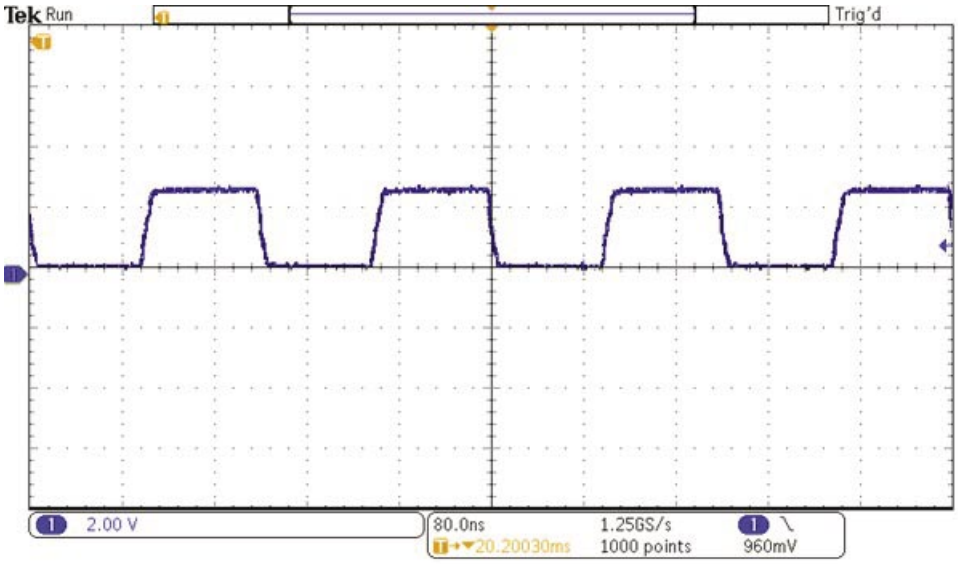


**Fig. 12. Result of myRIO output testing with no delay time**

The removal of the delay time block (which enables setting the "wait" time) caused, in the case of the cRIO controller, overlapping (merging) of the signal, resulting in the output signal being continuous. In the case of myRIO, the switching frequency obtained was 10 MHz (100 ns). In addition, it can be observed that falling and rising edges do not have the character of a unitary step (falling and rising slopes are noticeable).

The waveforms obtained reveal that the switching signals are too much distorted (both for cRIO and myRIO) to properly control the operation of a hybrid electromagnetic launcher with pneumatic assist.

In order to determine the minimum switching times of the cRIO controller with the NI 9474 module, it is necessary to reduce the resistance value between the digital output and ground (a resistance value of 330 Ω is sufficient for further testing).

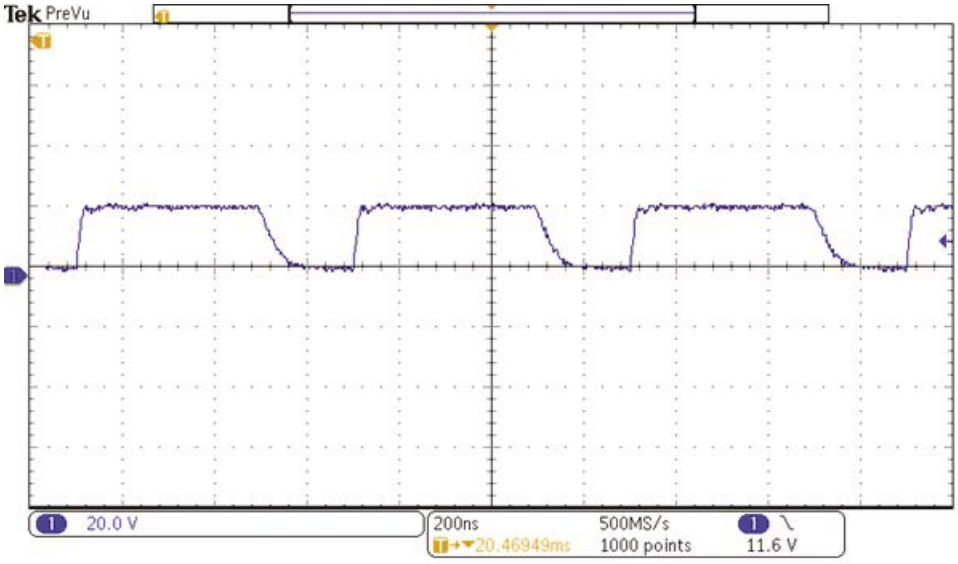


**Fig. 13. Result of myRIO output testing at minimum occupancy time**

Fig. 13 shows the recorded waveform for the minimum switching time (for the highest switching frequency of 4 MHz), which guarantees correct switching of the digital output (no state overlap effect).

### 2.3. Digital input switching time with output state tripped by FPGA

In the next stage of testing, the time was measured between the tripping of the physical digital output and the response on the second physical digital input of the signal value (logical 1 or 0).

For this purpose, the NI9423 digital input module was used, where the input update rate is 1 μs [13]. The physical arrangement of the electrical connections was made in such a way that the output of the digital module NI9474 was connected directly to the input of the NI9423 module.

Fig. 14 presents the program developed to verify the switching time, implemented at the FPGA level, for both tested controllers.

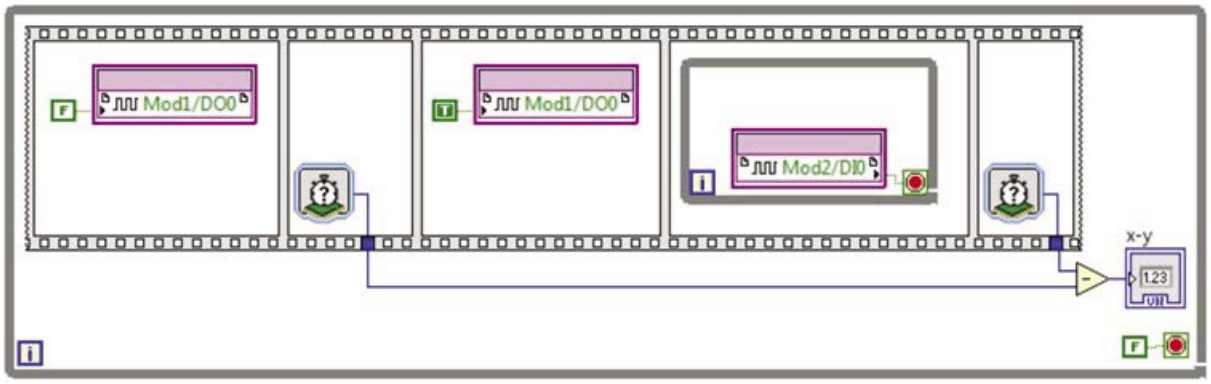


**Fig. 14. Program for testing switching time with tripping by FPGA**

The obtained results (readouts from the "x-y" block) are summarized in Table 3, in which the time needed to perform the first iteration of the program (program without the outer "while" loop) and the mean program execution time are given.

**Table 3.** Comparison of switching times / program execution tripped by FPGA

| Parameter | cRIO-9022 | myRIO-1900 |
|---|---|---|
| Mean time of first iteration | 150 ns (6.67 MHz) | 225 ns (4.4 MHz) |
| Mean execution time | 150 ns (6.67 MHz) | 225 ns (4.4 MHz) |

The results presented in Table 3 show that the industrial controller has a faster response time than the myRIO controller, despite the same processor frequency.

### 2.4. Digital input switching time with output state tripped by RT processor

Verification of the switching time induced by the RT processor was carried out in a similar way. A program was developed for this purpose and implemented in the RT module of both controllers. The program contains a part responsible for controlling the digital output and a loop that waits to receive the digital input signal (Fig. 15a). In order to physically control the digital output and input it is also necessary to develop a code fragment for the FPGA level (Fig. 15b).

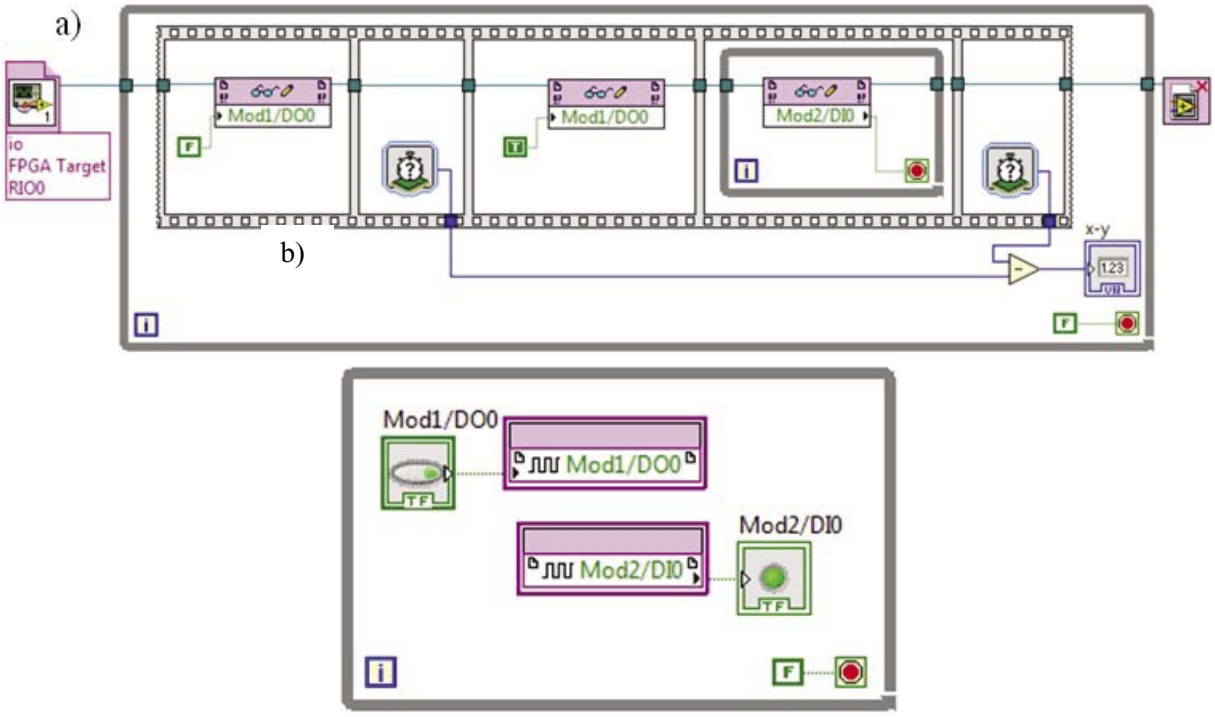


**Fig. 15. Program for testing switching time:**
a) for RT, b) for FPGA

The obtained results are summarized in Table 4, in which the time needed to perform the first iteration of the program (RT program without the outer "while" loop) and the mean time are given.

**Table 4.** Comparison of switching times / program execution

| Parameter | cRIO-9022 | myRIO-1900 |
|---|---|---|
| Mean time of first iteration | 28 µs (25.7 kHz) | 24 µs (41.7 kHz) |
| Mean execution time | 6 µs (166.7 kHz) | 8 µs (125 kHz) |

With tripping controlled at the RT processor level, it was again the cRIO controller that showed slightly shorter response times. However, note that the time of performing a single iteration is much longer than the continuous operation of the program in an infinite loop.

## 3. CONCLUSIONS

Comparison was made of some selected parameters of the cRIO-9022 (industrial controller) and myRIO-1900 (student device). The results of laboratory tests aimed at comparing the rise and fall time of the signal edge at the digital output for both controllers were presented. The study was conducted to assess the interchangeability of both controllers in the control system of a hybrid electromagnetic launcher with pneumatic assist.

The selected parameters of the cRIO-9022 (industrial controller) and myRIO-1900 (student device), edge rise and fall times on the digital output were compared, and the signal switching times were verified for two different cases: FPGA and RT processor tripping. These tests were carried out to assess the possibility of using (interchangeably) both of these controllers in the control and measurement system of the test stand with a hybrid electromagnetic launcher with pneumatic assist.

The laboratory tests carried out have shown that both tested controllers could be used in systems where the required maximum signal switching frequency is in the order of a few kHz.

It was also shown, in section 2, that the NI9474 module requires a current load of the output, and that the myRIO-1900 controller proved to be superior in the process of correct signal switching at the highest frequency. The authors are aware that connecting a load in the form of a resistor to the digital output may be insufficient in systems with such high operating frequencies, but they reckoned that this type of approach is sufficient for testing purposes. The tests conducted have shown that the time of program execution with tripping carried out by the RT processor varies considerably during one-time and continuous operation (3-4-fold); this has not been observed in the case of tripping by FPGA.

To summarize, it seems that the properties, declared by the manufacturer, of the FPGA embedded in the myRIO processor have been confirmed (they do not differ in terms of quality from those used in industrial controllers, e.g. cRIO). The cRIO controller enables controlling actuators in a wider range of voltages and is capable of operating under less favourable environmental conditions.

The presented results confirm that it is possible to use the myRIO-1900 controller in place of the current cRIO-9022 controller, installed on the test stand with a hybrid electromagnetic launcher with pneumatic assist. Further research will focus on adjusting the control voltage between the hybrid launcher and the my-RIO1900 controller as well as on measurement verification under real conditions (on the test stand with a hybrid electromagnetic launcher).

## 4. REFERENCES

[1] Andrade H. A., Hogg S., Ahrends S.: Making FPGAs accessible to Scientists and Engineers as Domain Expert Software Programmers with LabVIEW. W: 1st International Workshop on FPGAs for Software Programmers (FSP 2014), September, 2014, Munich, Germany 2014.

[2] Makowski T.: Koncepcja systemu sterowania hybrydową wyrzutnią elektromagnetyczną przy zastosowaniu sterownika czasu rzeczywistego. Informatyka Automatyka Pomiary w Gospodarce i Ochronie Środowiska nr 2/2017.

[3] Ponce-Cruz P., Molina A., MacCleery B.: Fuzzy Logic Type 1 and Type 2 Based on LabVIEW™ FPGA. Springer International Publishing, Switzerland 2016.

[4] http://www.ni.com/pl-pl/shop/select/compactrio-modules-category#facet:&productBeginIndex:0&orderBy:&pageView:grid&pageSize:&, [Retrieved: 15.05.2018].

[5] http://www.ni.com/white-paper/10894/en/, [Retrieved: 15.05.2018].

[6] http://www.ni.com/white-paper/52251/en/, [Retrieved: 15.05.2018].

[7] http://www.ni.com/white-paper/53031/en/, [Retrieved: 15.05.2018].

[8] http://www.ni.com/white-paper/9017/en/, [Retrieved: 15.05.2018].

[9] http://www.ni.com/pl-pl/shop/select/myrio-student-embedded-device, [Retrieved: 15.05.2018].

[10] USER MANUAL AND SPECIFICATIONS NI cRIO-9022 Intelligent Real-Time Embedded Controller for CompactRIO. 2015.

[11] USER MANUAL AND SPECIFICATIONS NI cRIO-9111/9112/9113/9114/ 9116/9118 CompactRIO Reconfigurable Embedded Chassis. 2016.

[12] DATASHEET NI 9474. 2016.

[13] DATASHEET NI 9423. 2015.

[14] USER GUIDE AND SPECIFICATIONS NI myRIO-1900. 2016.

[15] USER GUIDE AND SPECIFICATIONS NI myRIO-1950. 2013.